Evaluation of Analytical Approximation Methods for the Macroscopic Fundamental Diagram

Gabriel Tilg [a,*], Sasan Amini [a], Fritz Busch [a]

[a] *Technical University of Munich, Germany, Department of Civil, Geo and Environmental Engineering, Chair of Traffic Engineering and Control*

Abstract

The Macroscopic Fundamental Diagram (MFD) describes the relation of average network flow, density and speed in urban networks. It can be estimated based on empirical or simulation data, or approximated analytically. Two main analytical approximation methods to derive the MFD for arterial roads and urban networks exist at the moment. These are the method of cuts (MoC) and related approaches, as well as the stochastic approximation (SA). This paper systematically evaluates these methods including their most recent advancements for the case of an urban arterial MFD. Both approaches are evaluated based on a traffic data set for a segment of an arterial in the city of Munich, Germany. This data set includes loop detector and signal data for a typical working day. It is found that the deterministic MoC finds a more accurate upper bound for the MFD for the studied case. The estimation error of the stochastic method is about three times higher than the one of the deterministic method. However, the SA outperforms the MoC in approximating the free-flow branch of the MFD. The analysis of the discrepancies between the empirical and the analytical MFDs includes an investigation of the measurement bias and an in-depth sensitivity study of signal control and public transport operation related input parameters. This study is conducted as a Monte-Carlo-Simulation based on a Latin Hypercube sampling. Interestingly, it is found that applying the MoC for a high number of feasible green-to-cycle ratios predicts the empirical MFD well. Overall, it is concluded that the availability of signal data can improve the analytical approximation of the MFD even for a highly inhomogeneous arterial.

Keywords:
Macroscopic Fundamental Diagram (MFD), Traffic Flow Theory, Empirical Analysis, Sensitivity Analysis, Monte-Carlo-Simulation, Microscopic Simulation

1. Introduction

Modeling urban traffic has been a major concern since the early days of traffic research. Urbanization and the associated growth in demand increase the need for research on efficient models of urban traffic on a network-wide scale. Early studies date back to the 1960s (Godfrey, 1969; Herman and Prigogine, 1979; Mahmassani et al., 1987) in which the idea of a macroscopic network-level relation of traffic flow and accumulation was introduced. Later, Daganzo (2007) formulated a macroscopic relationship between the network-wide outflow and the aggregated accumulation. This was verified in Geroliminis and Daganzo

*Corresponding author.
E-mail addresses: gabriel.tilg@tum.de (Gabriel Tilg)., sasan.amini@tum.de (Sasan Amini)., fritz.busch@tum.de (Fritz Busch).

Accepted manuscript for Transportation Research Part C: Emerging Technologies.
 DOI: https://doi.org/10.1016/j.trc.2020.02.003

(2008) that investigated the existence of the macroscopic fundamental diagram (MFD) by linking the vehicle accumulation to the space-mean flow in a network. They found a well-defined and low-scatter relationship for homogeneous regions which is insensitive to small changes in demand for empirical data from Yokohama. Such a property makes the MFD a promising tool for a wide range of applications in urban traffic control and modeling. Studies analyzing such potential vary from gating (Keyvan-Ekbatani et al., 2012; Aboudolas and Geroliminis, 2013; Girault et al., 2016; Yang et al., 2018), pricing (Zheng et al., 2016), perimeter control (Geroliminis et al., 2012; Kouvelas et al., 2017; Zhong et al., 2018; Sirmatel and Geroliminis, 2018), routing (Yildirimoglu et al., 2018; Amini et al., 2018), the investigation of the impact of a network's topology on its performance (Knoop et al., 2014b; Ortigosa et al., 2017), to the analysis of the effects of parking on urban traffic dynamics (Cao and Menendez, 2015; Leclercq et al., 2017) and traffic control in a connected environment (Yang et al., 2019).

Inspired by the findings of Geroliminis and Daganzo (2008) several studies investigated the existence of a similar relationship in a number of cities around the world. This includes Yokohama, Japan (Geroliminis and Daganzo, 2008), Toulouse, France (Buisson and Ladier, 2009), Brisbane, Australia (Tsubota et al., 2014), Zurich, Switzerland (Ambühl et al., 2017), Lucerne, Switzerland and London in the United Kingdom (Ambühl et al., 2018), and many other cities (Loder et al., 2019). The data sets for these MFDs came mostly from loop detectors and probe vehicles. However, these data have to be treated with care as several biases are included. Methods to reduce the impact of these biases are reported in the literature (Ambühl et al., 2017; Du et al., 2016; Leclercq et al., 2014). Moreover, a heterogeneous density distribution might lead to hysteresis in the MFD (Geroliminis and Sun, 2011; Gayah and Daganzo, 2011; Saberi and Mahmassani, 2013; Shim et al., 2019; Ambühl et al., 2018). New technologies and associated data, such as mobile phone traces, can help to reduce the data measurement related biases.

Even though empirical observations are essential, they come with a number of limitations. First and foremost, they do not allow a systematic analysis of the characteristics of the MFD and the influential factors on its shape. Secondly, they require extensive data processing as real sensors are prone to failure, bias and incomplete coverage of the network. Thirdly, many cities do not possess empirical data and, hence, are not able to empirically derive the MFD. Thus, some simulation-based studies on MFD have been conducted. Generally speaking, the results of these studies (e.g. Duruisseau and Leclercq, 2018; Gayah et al., 2014; Knoop et al., 2014a; Ji et al., 2010) show that the MFD depends on link characteristics, the network topology, traffic control, and route choice.

Despite the fact that simulation studies show promising results, the application of large-scale simulations might be limited due to the burdensome calibration. Additionally, if the application of the MFD is aiming towards real-time evaluation of traffic control measures, the high computational cost of simulation-based methods might reduce their suitability. However, existing analytical methods rectify these drawbacks of simulation-based and empirical estimation of the MFD. These methods are mainly based on the framework of the variational theory (VT) (Daganzo, 2005a,b; Daganzo and Menendez, 2005). The corresponding concept is described by Daganzo and Geroliminis (2008), who introduced the method of cuts (MoC) that is able to find an upper bound for the arterial MFD. Leclercq and Geroliminis (2013) continued this line of research, improved the MoC and showed the effects of route choice on a simple network. The concept was further enhanced by Daganzo and Lehe (2016), who formulated the method as a linear program. Contrarily to this deterministic approach, Laval and Castrillón (2015) developed a stochastic analytical method based on the MoC and the renewal theory, called stochastic approximation (SA) hereafter. The method enables to approximate the MFD for urban arterial roads as well as networks. The authors found the MFD mainly to be influenced by the mean-block-length-to-green ratio and the mean-red-to-green ratio.

Analytical methods are particularly suitable to run extensive sensitivity analyses which provide insights on the impact of certain parameters on the shape of the MFD. For example, Geroliminis and Boyacı (2012) investigated the effects of different traffic signal offsets and link lengths on the MFD. Daganzo et al. (2018) studied the impact of adaptive signal offsets on the MFD. Moreover, these methods allow the performance of an ex-ante prediction of the MFD. Such a prediction is crucial for the applicability of MFD-based modeling techniques. For instance, Ambühl et al. (2018) developed a method to derive a functional form with a physical meaning for the MFD. They state that next to empirical data, also analytically derived MFDs can deliver essential input to the estimation of the functional form. Moreover, Mariotte et al. (2017) analyzed

different ways to derive the outflow from regions in which traffic dynamics are described based on an MFD. This input MFD can be derived based on analytical approximations. Mariotte and Leclercq (2019) proposed a new flow transfer scheme that considers multiple trip lengths in one region. Batista et al. (2019) developed a methodology for adapting trip lengths for multi-regional MFD-based applications. The methodology of both works requires MFDs as input which can be derived analytically.

These works confirm the importance of analytical approximation methods in MFD-based modeling of urban traffic. Naturally, this leads to the question of how well empirically derived MFDs can be approximated. The original method of practical cuts (Daganzo and Geroliminis, 2008) and the SA (Laval and Castrillón, 2015) have both been validated with data from Yokohama, Japan. However, to the best knowledge of the authors, no such verification has been reported for the MoC for inhomogeneous arterials, nor has the SA been directly compared to the MoC for such an arterial. Additionally, many advances on empirical MFD estimation methods have been achieved to date, which were not considered in these studies. Signal data is an input for both analytical approximation methods. Yet, no information on detailed signal data is available for the case of Yokohama. Therefore, it remains unclear to what extent the existence of such data can improve the estimation accuracy of the analytical methods. Furthermore, extensions to consider the effects of public transport operation exist for both methods (Xie et al., 2013; Castrillon and Laval, 2017). Nonetheless, no reports about any evaluation of them based on comparison to empirical data are known.

This paper aims to address the mentioned research gaps by comparing the MoC and the SA including the most recent extension to consider public transport operation to an empirically derived arterial MFD. Even though the SA applies to networks, the MoC was originally developed for arterials. Thus, we choose an arterial for this study. The empirical data at hand consists of loop detector data (LDD) and signal data. The LDD come from an inhomogeneous road segment in Munich, Germany, with multi-modal traffic, active actuated signal control, and transit signal priority. The occurring modes include private cars and buses, trams on physically separated tracks and bicycle traffic on bike lanes. This allows investigating the effects of infrastructure complexity on differences between empirically and analytically derived MFDs. The three dimensional passenger MFD (e.g. Geroliminis et al. 2014; Loder et al. 2017) extends the idea of the MFD to multi-modal systems. It relates the passenger production to the network bus and car accumulation. However, such an analysis requires additional data and lies beyond the scope of this paper. Thus, we focus on the 2D-MFD approximated by the MoC and the SA including their public transport extensions. Thereby, we compare the according results to empirical data from the arterial in Munich. The results of this comparison are thoroughly analyzed. We set the focus on the measurement bias inevitably included in LDD, the signal data and the impact of public transport operation. No comparison of the analytical methods including the public transport extension has been conducted so far. Also, no investigation of the role and benefit of a rich signal data set to accurately estimate the MFD has been reported. Lastly, to the best knowledge of the authors, no attempts to quantify the effects of these elements on the difference between empirical and analytically approximated MFDs have been presented. Interestingly, the results of this paper indicate that applying the MoC for a wide range of signal data leads to an aggregated traffic pattern close to the empirical MFD. This is the main contribution of this paper. As an overall result, this study sheds light on the performance of the studied analytical approximation methods, as well as on the importance of corresponding assumptions and simplifications.

The remainder of the paper is structured as follows. Section 2 describes the underlying theory of the MoC and the SA. Moreover, the current state of research regarding the empirical MFD estimation is presented. Section 3 specifies the general methodology of the paper including a case study, the applied methods, the investigation of the measurement bias and the sensitivity analysis of input parameters related to signal control and public transport operation. The results of the case study and their discussion are presented in Section 4. Furthermore, the section includes the results of the investigation of the measurement bias based on a microscopic simulation in SUMO (Lopez et al., 2018), and of the sensitivity analysis of the analytical approximations. Finally, Section 5 draws closing conclusions, highlights limitations and outlines possible future research. To increase the readability of the paper, we provide a list of abbreviations used throughout the paper in alphabetical order in Table 1.

Table 1: List of abbreviations

Abbreviation	Term
BVP	Boundary value problem
CDF	Cumulative distribution function
ELDD	Empirical loop detector data
FCD	Floating car data
FD	Fundamental diagram
IVP	Initial value problem
KWT	Kinematic wave theory
LDD	Loop detector data
LOESS	Locally estimated scatter plot smoothing
MFD	Macroscopic fundamental diagram
MoC	Method of cuts
OD	Origin-Destination
RMSE	Root Mean Square Error
SA	Stochastic approximation
VFCD	Virtual floating car data
VLDD	Virtual loop detector data
VT	Variational theory

2. MFD estimation

This section describes analytical approximation and empirical estimation methods to derive the MFD. More specifically, the frameworks of the MoC and the SA are introduced as main representatives of analytical approximations. Besides, important aspects and related research of empirical MFD estimation are presented. This section as well as the following one include many variables. For the sake of clarity, a nomenclature including these variables is provided in Table 2.

Table 2: Nomenclature

Fundamental diagram		
u	[km/h]	Free flow speed
w	[km/h]	Backward wave speed
k_j	[veh/km]	Jam density
q_{cap}	[veh/h]	Capacity
Variational theory		
x	[km]	Spatial dimension
t	[h]	Temporal dimension
$P(x,t)$	[-]	Generic point at (x,t)
$N(P)$	[veh]	Cumulative vehicle count at $P(x,t)$
$\mathcal{B}_P$	[-]	Boundary data in the domain of dependence of P
Δ_{BP}	[veh]	Maximum number of vehicles that can pass a moving observer which travels from B to P
Method of cuts		
q	[veh/h]	Flow
k	[veh/km]	Density

Table 2: Nomenclature (continued)

$Q(k)$	[veh/h]	MFD
j	[-]	Index of cut C
C_j	[-]	Cut
v_j	[km/h]	Mean speed of cut C_j
$R(v_j)$	[veh/h]	Costs of cut C_j
v_b	[km/h]	Average speed of buses
Stochastic approximation		
v_O	[km/h]	Speed of moving observer
q	[veh/h]	Flow
k	[veh/km]	Density
k'	[-]	Dimensionless density
μ_g	[s]	Mean green time
μ_r	[s]	Mean red time
ρ	[-]	Long-run red to green ratio
μ_l	[m]	Mean block lengths
λ	[-]	Mean dimensionless block length
δ	[-]	Average coefficient of variation
$F_{q(k')}(q)$	[veh/h]	CDF of the MFD
s_0	[-]	Strategy related to $v_O = 0$
$\Omega = \{s_1, s_2\}$	[-]	Strategies related to $v_O = [u, w]$
B	[-]	Number of intersections
p_s	[-]	Probability that bus stops within a link
u_b	[km/h]	Average bus free flow speed
t_d	[s]	Average dwell times of buses
Sensitivity analysis		
n	[-]	Number of sample variations for Monte-Carlo-Simulation
q_{min}	[veh/h]	Minimum of n results for $Q(k)$
q_{mean}	[veh/h]	Mean of n results for $Q(k)$
q_{max}	[veh/h]	Maximum of n results for $Q(k)$

2.1. Analytical approximation methods

In general, the herein described analytical approximations of the MFD are based on the VT. The VT enables to calculate the exact solutions of an initial or boundary value problem (IVP or BVP, respectively) according to the kinematic wave theory (KWT) (Lighthill and Whitham, 1955; Richards, 1956). The VT states that a kinematic wave problem can be solved as shortest path problem in the time-space plane. The corresponding costs are related the boundary data and the maximum number of vehicles that can pass a moving observer traveling along a given path. The mathematical formulation is:

$$N(P) = \inf_{B \in \mathcal{B}_P} \{N(B) + \Delta_{BP}\} \tag{1}$$

where $N(P)$ is the cumulative count of vehicles at the generic point $P(x, t)$, $\mathcal{B}_P$ is the boundary data in the domain of dependence of P, Δ_{BP} is the maximum number of vehicles that can pass a moving observer which travels from the point B on the boundary to P. For more details, please refer to Daganzo (2005a,b) and Daganzo and Menendez (2005).

2.1.1. Method of cuts

Daganzo and Geroliminis (2008) introduced a methodology to analytically approximate the MFD for homogeneous arterials with identical block lengths and signal control parameters. This methodology was further extended by Leclercq and Geroliminis (2013) to be applicable to heterogeneous topologies.

In order to set up an IVP several input parameters need to be specified. These include the number of links in the arterial, the number of lanes on and the length of each link, signal parameters and the fundamental diagram (FD). This defines the solution space and consequently the shortest path problem. The solution space in the (t, x)-plane consists of horizontal edges representing intersections including both green and red phases. Note that green times and cycle lengths are not allowed to vary within a specific intersection. In other words, only fixed time signal control can be modeled. Additionally, slanted edges with extremal slopes (free flow speed u or backward wave speed w) starting at bottleneck termini connect the horizontal edges related to different intersections. Whenever such a slanted edge hits a red phase, it is terminated. Based on the slope of these edges, costs for each edge can be defined. The corresponding values are derived based on the VT and relate to the maximum passing rate a moving observer would observe traveling along such an edge. This procedure leads to a numerical representation of a kinematic wave problem which is called global variational graph (Leclercq and Geroliminis, 2013).

Depending on the initial density, the flow at a certain point approaches a location-dependent limit for the case of a steady state. Daganzo and Geroliminis (2008) describe this flow based on Eq. (1) as $q = N(P)/t, t = t_0 \to \infty$. Thus, an upper bound of the flow q can be derived for each k by evaluating Eq. (2) based on the global variational graph as follows:

$$q = \inf_{v_j} \{k v_j + R(v_j)\} \tag{2}$$

with $q = Q(k)$ as the MFD, k as the density, v_j as the average speed of a moving observer j and $R(v_j) = \Delta_{BP}/t, t = t_0 \to \infty$ as the related maximum passing rate.

Evaluating Eq. (2) for several k and a specific moving observer with average speed v_j leads to a constraint of the flow q along with the evaluated range k. Repeating this procedure for several different average moving observer speeds v_j results in a family of cuts. The lower envelope of all cuts is the MFD $Q(k)$.

The original method (Daganzo and Geroliminis, 2008) is only applicable on homogeneous arterials which herein means that block lengths, green times and cycle lengths do not differ between intersections. Even though no signal data were available, the results of the analytical approximation fit an empirical MFD for the city of Yokohama. The authors stated that differences in the predicted and the measured MFD were due to inhomogeneity in the network and errors in the data. However, as Daganzo and Lehe (2016) pointed out, this method does not necessarily lead to a tight bound for stationary cuts, which relate to an average moving observer speed of $v_j = 0$. The authors rectified this drawback and formulated the overall method as a linear program. Nevertheless, their approach to estimating a tight bound for stationary observers is transferable to the MoC.

Xie et al. (2013) further extended the MoC to approximate the effects of public transport vehicles on the capacity of an arterial. The additional input parameters consist of the average bus speed v_b and the headways. The effects of buses are modeled based on the numerical representation of moving bottlenecks. A moving bottleneck is approximated by reducing the capacity of a certain link. That is, the costs of the corresponding green phase edges at the upstream and downstream intersection are adjusted. Thus, the effects of public transport can be included in the variational graph and the remaining procedure to derive cuts does not need to be adjusted.

2.1.2. Stochastic approximation

A different approach is presented by Laval and Castrillón (2015). They introduced the SA of the MFD for urban arterials and networks. Again, the core of the method is based on the VT and the MoC. Three types of cuts are evaluated. They are associated with different strategies which are explained in the following. Strategy s_0 is related to a stationary observer with a mean moving observer speed $v_O = 0$. Strategy s_1 relates to moving observers traveling with speed $v_O = [u, w]$ which stop when they cross a red phase. There they travel horizontally to the beginning of the current red phase. From there they resume the speed of

$v_O = [u, w]$ until the next red phase is hit. Strategy s_2 is similar except for the fact that moving observers stop at every intersection independently if they cross a green or red phase. The fundamental difference of this method compared to the MoC is that the duration of green phases and cycle lengths do not have to be regular for its application. Thus, not only fixed time control settings can be analyzed but also networks or arterials where adaptive or actuated signal control is active.

An additional element of this framework is the transformation of the FD from the (q, k)-plane to a (q, k')-plane, where k' is the normalized density. This procedure leads to a symmetric and normalized FD. Thus, the related parameters are only required for the transformation back to the (q, k)-plane but not for the general application of the method. The only necessary input parameters are the mean green μ_g and mean red μ_r times, the mean block length μ_l and the related coefficients of variation δ which are assumed to be equal for simplicity. Based on these input parameters and the renewal reward theory, a framework is built to estimate the mean and coefficient of variation for cuts related to the described strategies. Assuming a normal distribution for the cuts, this framework enables to calculate a cumulative distribution function (CDF) for each cut and eventually for the MFD. Thus, it allows specifying certain percentiles of the MFD at (q, k)-pairs and therefore to derive its stochastic representation. Mathematically, the CDF of the MFD is expressed as shown in Eq.(3).

$$F_{q(k')}(q) = 1 - (1 - F_{s_0}(q))^B \prod_{s \in \Omega} (1 - F_{s,k'}(q)) \tag{3}$$

where $F_{q(k')}(q)$ denotes the CDF of the MFD, q the flow, k' the normalized density, s_0 and $\Omega = \{s_1, s_2\}$ the different strategies and B the number of intersections. More details on the mathematical framework can be found in Laval and Castrillón (2015).

Major arterials in urban networks are often frequented by public transport vehicles. Possible impacts of multimodal traffic on the stochastic representation of the MFD for homogeneous arterials were reported in Castrillon and Laval (2017). In this case, homogeneity refers to equal signal parameters and block lengths amongst the modeled intersections. The authors modified the SA to analytically approximate these impacts and introduce three new parameters, the average bus free flow speed u_b, the stop probability p_s and the average bus dwell time t_d. Castrillon (2015) presented an extension of this method for heterogeneous arterials. This is done by adjusting model parameters to account for the stationary bottleneck effect of buses as well as for their role as moving bottleneck.

2.2. Empirical estimation methods

Next to analytical approaches, the MFD can be estimated based on data from fixed sensors or probe vehicles. This section presents related estimation techniques, and which drawbacks come with associated data sources. However, potential ways of dealing with such drawbacks are not listed here. Instead, we refer to the corresponding studies. Eventually, we discuss the assumption of homogeneously distributed congestion as it has substantial effects on the shape of the MFD.

2.2.1. Data types

Loop detectors measure vehicle counts and the duration they are occupied. The data are often aggregated to 3- or 5-minute intervals. Thus, average flows during these intervals, as well as occupancy values in percent can be derived. LDD might be faulty since malfunctions might occur during operation. Data recording systems apply basic algorithms which help to exclude the majority of technology-induced measurement errors. The first MFD based on LDD was shown in Geroliminis and Daganzo (2008). It was derived by averaging the link-weighted network density and flow. Even though a well-defined MFD was found for that case, empirical MFDs have to be treated with care as several biases were identified associated with LDD in the literature. For example, Wu et al. (2011) showed that high scatter in the MFD for an arterial road can result from the fact that loop detectors also capture transient states. Ambühl et al. (2017) described the loop detector placement bias. It refers to the fact that loop detectors only measure traffic states at a specific position, which is then often regarded as representative for the entire link. In addition, Courbon

and Leclercq (2011) argued that loop detector positions need to be distributed uniformly across the links of the network to represent average traffic states on a global level. Zockaie et al. (2018) found that not only the position of loop detectors is crucial, but also the link selection plays an important role for the estimation of the MFD. This is because the measured traffic on selected links is related to Origin-Destination (OD) pairs. For a valid MFD estimation, these ODs have to represent the overall OD distribution in the network. Another bias associated with the link selection was described in Ambühl et al. (2017). The authors argued that loop detectors are usually installed on links more prone to congestion. Thus, this might result in an overestimation of network-wide congestion. Despite these biases, LDD are a commonly utilized data type for the MFD estimation due to their high availability compared to other data types.

As mentioned before, probe vehicles can be an alternative data source to estimate the MFD (e.g. Geroliminis and Daganzo, 2008). These data come either from GPS devices, mobile phones or are the result of processed Bluetooth data (e.g. Tsubota et al., 2014) and are often referred to as floating car data (FCD). They are considered to represent a better spatial coverage of traffic states in the network (Nagle and Gayah, 2014). Leclercq et al. (2014) showed that the MFD estimation based on probe vehicle data is more accurate than based on loop detectors. However, a crucial element is the penetration rate. It describes the relative number of probe vehicles in the total flow which is difficult to estimate for empirical data but essential for the MFD estimation. A potential way to cope with this drawback was shown by Nagle and Gayah (2014) who fused FCD with limited LDD for MFD estimation. However, they assumed that probe vehicles are uniformly distributed throughout the network. This might not be true since these data often come from certain vehicle types (e.g. taxi data) which might drive only on specific routes and thus biases might be introduced. Consequently, this leads to a heterogeneous distribution of trajectories. Du et al. (2016) investigated the effects of such heterogeneously distributed FCD on the MFD including data from probe vehicles with varying trip lengths. More analyses of the fusion of LDD and FCD for MFD estimation is reported in Zockaie et al. (2018) and Ambühl and Menendez (2016). Furthermore, Dakic and Menendez (2018) showed that data from automated vehicle location devices installed in public transport vehicles can contribute to the empirical MFD estimation.

Another kind of situation occurs for the case of microscopic simulation data. Under these circumstances, all vehicle trajectories are known and can be extracted. This enables to calculate the average flow, density and speed based on Edie's definition (Edie, 1963), which was referred to as Edie method in Leclercq et al. (2014). In such a case, no measurement biases are included in the data. Saberi et al. (2014) showed the existence of the MFD for a microscopic simulation of Chicago, Illinois, and Salt Lake City, Utah. They concluded that even without any measurement biases, the MFD still shows a range of flows for a given density. More specifically, they presented a hysteresis pattern in the MFD which occurs due to inhomogeneous congestion in the network.

2.2.2. Network homogeneity

The previous paragraphs describe the existing data sources for the estimation of the empirical MFD, as well as associated biases. Early works exploring the effects of heterogeneity in urban and freeway traffic networks on the MFD are Buisson and Ladier (2009); Mazloumian et al. (2010); Geroliminis and Sun (2011); Knoop et al. (2015) and Saberi and Mahmassani (2013). Even for the case of simulated and thus bias-free data, scatter in the MFD might still occur (Saberi et al., 2014). Based on empirical data, Ambühl et al. (2018) suggest several reasons for this. First, the heterogeneous spatial distribution of traffic density is supposedly a main factor. The MFD in its original definition is merely found for homogeneously congested networks. In reality, however, this is rarely observed. Flows measured during inhomogeneously distributed densities are lower than in the homogeneous case (e.g. Daganzo et al., 2011; Mühlich et al., 2014; Knoop et al., 2015). It was found that the partitioning of large-scale networks into regional sub-networks can substantially decrease the heterogeneity of congestion in these smaller networks. Clustering methods for this partitioning are discussed in Saeedmanesh and Geroliminis (2016); Lopez et al. (2017); Saeedmanesh and Geroliminis (2017); Ambühl et al. (2019). Secondly, the MFD is merely well-defined for steady states. However, changes in traffic states do not propagate instantaneously throughout the network. These dynamics can lead to multiple flows for specific density measurements (Mariotte et al., 2017). Lastly, public transport

operation might have different impacts on traffic flow throughout the day (e.g. Arnet et al., 2015; Castrillon and Laval, 2017).

3. Methodology

This paper aims to perform an up-to-date evaluation of the existing methods to analytically approximate the MFD. A preliminary analysis for a data set of one working day of a road segment of Munich showed that the occurring differences cannot be explained by a simple scenario-specific evaluation (Tilg et al., 2019). Thus, a more sophisticated approach is proposed in this paper. The framework for the general methodology is shown in Figure 1.

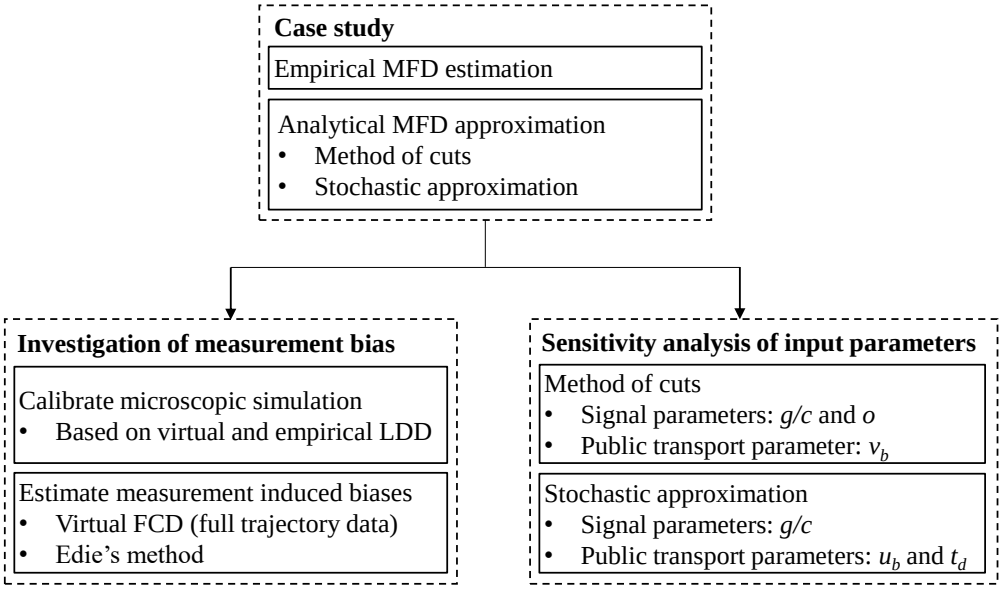

Figure 1: General methodological framework.

First, a case study based on a segment of the urban arterial Leopoldstraße located in the city of Munich, Germany, is conducted. The choice of an arterial road seems to be appropriate for this study since the MoC was originally developed for arterials. Thus, we minimize possible error sources by focusing on such an arterial. The analytical approximation (MoC and SA) and empirical estimation methods are applied based on data recorded on this road. The purpose of this case study is to investigate the fit of the analytical MFD approximations to the empirical MFD. Furthermore, it is the starting point for a systematic study of the appearing differences between the resulting MFDs.

As mentioned before LDD include a measurement bias that can affect the empirical derived MFD and thus also influence the difference to analytical approximated MFDs. Thus, a second step is to investigate this measurement bias. This is done by the means of microscopic simulation. The calibration of the simulation is carried out based on empirical and virtual LDD. To estimate the bias-free MFD, virtual trajectory data are used to calculate average flow and density according to Edie's method as shown in Leclercq et al. (2014). Based on the resulting bias-free MFD, the nature of the measurement bias can be analyzed.

Lastly, the role of signal data and public transport operation on the approximated MFD shape is investigated. The analytical methods and related input parameters imply certain simplifications of reality. The explicit studied parameters are explained below. The study is conducted as a sensitivity analysis based on a Monte-Carlo-Simulation for both analytical approximation methods. This study allows investigating the role of input parameters and analyzing the corresponding results in comparison to the empirical MFD.

The remaining section describes the layout of the case study, applied analytical approximation methods

as well as the empirical MFD estimation, the investigation of the measurement bias, and the structure of the sensitivity analysis.

3.1. Case study

The Leopoldstraße leads from the center to the very north of Munich and serves as a critical corridor that connects the city center to the city's ring road. The empirical data containing raw LDD and signal data were collected from a segment of the northbound Leopoldstraße on a typical working day in October 2017. Comparable results for the time series of occupancies are found for other weekdays at the Leopoldstraße. Additionally, the distribution of green times and cycle lengths in a second available data set do not substantially differ to the one shown in the paper. Thus, we assume that analyzing the data presented in the paper is representative for the given road segment. Figure 2 shows the layout of the studied road segment with a total length of 1.1 km. It includes five signalized intersections, labeled from one to five in the figure. The studied segment mostly consists of two lanes except for some of the intersections where a dedicated turning lane exists for right or left turning vehicles. The loop detectors on the turning lanes are stop-line detectors, which cannot be directly used to derive the MFD, and therefore, are not considered in this study. As it can be seen in Figure 2, there are some minor unsignalized intersections along the arterial from which no data, i.e. number of turning and incoming vehicles, were available. For the sake of simplicity, the impact of these intersections is neglected.

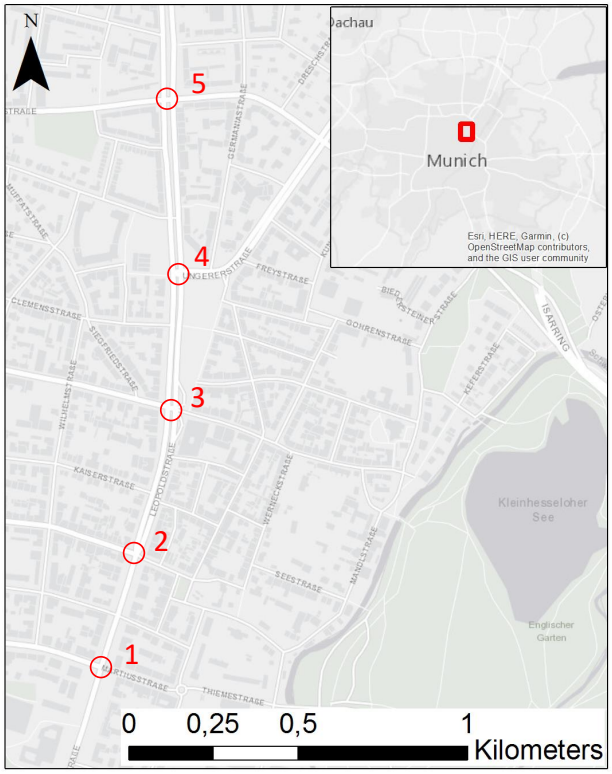

Figure 2: The urban arterial Leopoldstraße in Munich, Germany. The numbers 1-5 refer to the examined intersections and increase in direction of travel.

Each of the five intersections is controlled by actuated traffic signals i.e. adaptive green time and cycle lengths as well as prioritized public transit vehicles. Right at the north-east corner of intersection 3 an important mobility hub, called *Münchner Freiheit*, i.e. a transfer point for public transport users between bus, tram, metro and car-sharing vehicles, is located. Moreover, another on-street bus stop is located

between intersection 1 and 2. Two bus lines operate on the arterial, each with a 10-minute headway during most times of the day. Additionally, a tram line operates from intersection 3 to 5. However, the tram tracks are physically separated from the other lanes and thus do not impact traffic flow on the neighbouring lanes.

3.2. MFD estimation

The MoC and the SA are applied on the described road segment of the Leopoldstraße. Furthermore, an empirical MFD is estimated as described below. The quantitative comparison is made based on the root mean squared error (RMSE), which was successfully applied in the terms of MFD-related research (e.g. Ambühl et al. 2018).

3.2.1. Empirical estimation

The estimation of the empirical MFD for the case study is based on data recorded from loop detectors. Upstream of each intersection a loop detector is installed on each lane. In total, that sums up to 10 loop detectors for the northbound travel direction. All considered loop detectors are installed approximately 35 meters upstream of the stop-line. The average length of a loop detector is 1.5 m. Each observation consists of a time-stamp and an occupancy duration. A set of plausibility tests such as searching for duplicate detections, negative headways, and extreme occupancy values is performed. Subsequently, the data are aggregated in 5-minute intervals. The result is a vehicle count and an occupancy value for each detector for each interval. In order to reduce the noise and errors due to aggregation, as well as to exclude outliers, we smooth the data using time series analysis as suggested in Ambühl et al. (2018). Then, the obtained occupancies are used to calculate densities assuming an average vehicle length of 5 meters. The density is calculated based on the sum of the mean vehicle and detector length (see Ambühl et al. 2018).

Another data type available is signal data. This includes the time-stamp for each phase change, as well as the phase type (green, amber or red) for all intersections. Since the traffic signals are not pre-time controlled, the cycle lengths, green times and red times are strongly skewed. Figure 3 shows boxplots for green times and cycle lengths of the northbound leg at each intersection for the measurement day. The ordinate shows the duration of the corresponding parameter in seconds. The intersection labels are displayed on the abscissa. As it is shown in the plots, substantial variance of both parameters can be observed. The

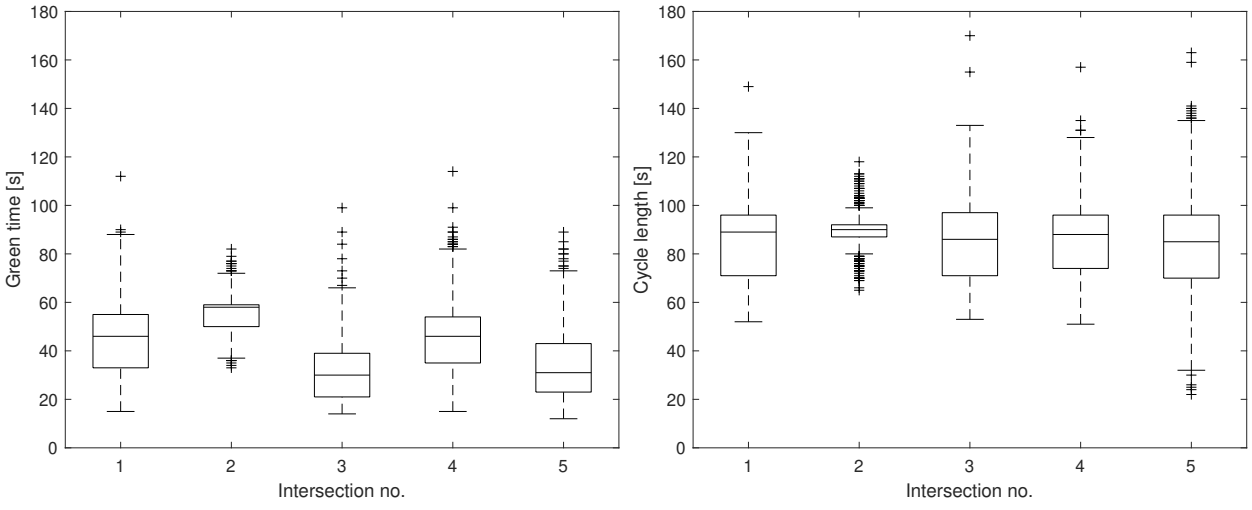

a) Green times [s] **b)** Cycle lengths [s]

Figure 3: Green times and cycle lengths for the studied intersections at Leopoldstraße (October, 2017).

reasons for this variance are the actuated traffic signal control, the transit signal priority, and the fact that the green times and cycle lengths of the entire day and thus different signal plans are included in

the illustration. Additionally, it can be observed that the scatter is higher for longer green times. This is possibly due to the required minimum green times at the studied intersection legs. On the contrary, the distribution of cycle lengths seems to be symmetric. Moreover, the majority of green times of intersection 3 and 5 are substantially lower than the ones at the other intersections. Regarding intersection 3, this could be explained by the fact that it is located next to the *Münchner Freiheit* mobility hub, where many bus and tram lines stop. Thus, the effect of transit signal priority is very strong. Possible reasons for a lower mean green time at intersection 5 are the that a tram line crosses the intersection, and a bus line is running between the east- and southbound leg of the intersection. Both are having priority and thus green times are reduced for private vehicles.

Furthermore, limited historical FCD are available. The data are too scarce to benefit from merging it with LDD for the empirical MFD estimation. However, it can be used to estimate the free flow speed u as explained below.

3.2.2. Method of cuts

The first analytical approximation for the MFD which is evaluated is the MoC. As described in Section 2, a global variational graph needs to be constructed to apply this method. For this purpose, the link FD, the arterial topology, the signal timings and the average bus speed v_b need to be defined.

The link FD plays an important role for the MoC. To define it, three out of the four related parameters, the free flow speed u, the capacity q_{cap}, the backward wave speed w and the jam density k_j have to be specified. It has a crucial impact on the approximation of the MFD. The free flow speed u is chosen according to FCD which were available for the entire analyzed segment of the Leopoldstraße. The found value for the free flow speed equals $u = 45\,\mathrm{km/h}$. The jam density is assumed to be $k_j = 150\,\mathrm{veh/km}$. This is based on visual inspection of a number of queues captured by high-resolution aerial pictures. The backward wave speed is assumed to be $w = 15\,\mathrm{km/h}$. Leclercq (2005) report similar values for urban roads in Toulouse, France. In this study, however, the jam density is found to be substantially higher. Thus, we choose a slightly larger value for w to calculate realistic values for the capacity q_{cap}. Given these three parameters and assuming a triangular FD, the capacity is calculated as about $q_{cap} = 1690\,\mathrm{veh/h}$.

The block lengths are measured from OpenStreetMap® (OpenStreetMap contributors, 2019) and are defined as the segment length between two consecutive signalized intersections. The effects of the minor intersection along the arterial are neglected for this study. This is due to the fact that the analytical approximation methods are not capable of considering the impact of such intersections. Also, the corresponding streets are of a minor level and partly only one-lane streets. Furthermore, no flow or occupancy data from these streets are available. As shown in Figure 3, the green times and the cycle lengths are strongly skewed for all intersections. However, the MoC allows only for one value per intersection. In other words, only fixed time signal control can be modelled. Thus, we choose the average for both green times and cycle lengths for the case study. For the sensitivity study, a different approach is chosen as described below.

The last family of input parameters regards to public transport operation. The multimodal extension of the MoC (Xie et al., 2013) only needs an exogenous average bus speed as input parameter. As a first assumption, we choose 75 % of the car free flow speed which equals to $v_b = 34\,\mathrm{km/h}$ since no more accurate data is available. This value is based on a study of free flow speeds of different vehicle classes for Great Britain (Department for Transport, 2015). The ratio of car and bus free flow speeds in urban areas with a speed limit of about 50 km/h is 90 %. Taking into account that there exists one on-street bus stop on the studied arterial, and assuming a dwell time of 30 s, a bus speed v_b of 75 % of the car free flow speed u seems to be appropriate. However, the impact of this assumption is investigated as part of the sensitivity study. The dwell time of 30 s on average are chosen according to limited data from other bus lines which were recorded with GPS trackers.

Based on these input parameters a variational graph can be constructed. It allows deriving cuts C_j with speed v_j and costs $R(v_j)$ to estimate an upper bound for the arterial MFD. Since the Leopoldstraße represents a highly inhomogeneous arterial, an appropriate calculation time window is chosen to generate a sufficiently large solution space. Next, all possible moving observers are taken into account. For cuts with the same speeds, the ones with the lowest costs are chosen. The large size of the calculation time window

ensures that all possible paths are found. Finally, taking the lower envelope of all cuts leads to an estimate of the upper bound for the MFD on the given arterial.

3.2.3. Stochastic Approximation

The SA is the second method being evaluated. Again, the input parameters are derived based on the road topology, signal data and available public transport data.

The FD is not necessarily required to apply the SA. However, in order to compare the resulting MFD to the empirical and the MoC-based one, an FD is needed. The same values for the free flow speed u, the backward wave speed w, the jam density k_j and consequently the capacity q_{cap} are applied.

Furthermore, the block length is an input for the SA as well. The specific input parameter is the mean dimensionless block length $\lambda = 6.8$. The number of blocks in the studied road segment is $B = 5$. Theoretically, the SA allows to consider distributed green times and cycle lengths. The related input parameters are the average green time $\mu_g = 42\,\mathrm{s}$, and the long-run red to green ratio $\rho = 1.2$. Averaging the coefficient of variation of the green times, the red times and the block length results in an overall average coefficient of variation equals $\delta = 0.21$. No offset parameter is necessary as input for the SA.

The public transport extension of the SA requires additional input parameters. In the contrary to the MoC, the bus free flow speed is not assumed to account for potential stops. They are modelled explicitly via the stop probability p_s. Since there is a on-street bus stop only on one of the five segments, we choose $p_s = 1/5$. The average free flow bus speed u_b is chosen as 90 % of the car free flow speed, see the explanation in Section 3.2.2. Again, the average dwell time is $t_d = 30\,\mathrm{s}$.

Based on these parameters the mean and coefficient of variation for the cuts related to three different strategies can be calculated (see Section 2). Assuming normally distributed cuts, the CDF for each cut is defined. This enables to compute the CDF and thus the percentiles of interest for the MFD for the herein studied arterial road.

3.3. Investigation of the measurement bias

A measurement bias inevitably exists in LDD, as the data are recorded at fixed positions. There are certain procedures to minimize this bias, as described in Section 2.2. For example, measurements from several fixed sensors on different positions could be projected to a virtual link. These projected and then accordingly weighted measurements could lead to a reduced bias in the data. However, this is infeasible for the case studied in this paper since all loop detectors are positioned at nearly the same distance from the stop-line. Another way to exclude measurement induced biases is to gain complete knowledge about the traffic situation, i.e. all trajectories. Since this is not possible for the empirical data of the Leopoldstraße, a microscopic simulation environment is built in SUMO. The layout of the simulation assembles the real arterial. In total, 129 OD pairs are defined and the route choice is designed based on recorded turning rates at each intersection. Additionally, two public transport bus lines each with a headway of ten minutes are represented in the simulation. The estimation of OD pairs and input demand curves for each pair is based on the measured travel times. More details regarding that are described in Grigoropoulos et al. (2018).

In order to investigate the measurement bias, a calibrated microscopic simulation is needed. This is achieved by adapting the Krauss car-following model (Krauß, 1998) parameters with the objective of minimizing the difference between the two MFDs from real loop detectors and virtual detectors from the simulation. For this purpose, flow and density measurements are recorded at positions that correspond to the loop detector positions at the real Leopoldstraße. Based on these virtual LDD measurements a locally estimated scatter plot smoothing (LOESS) regression (Cleveland, 1979) is applied. Additionally, a LOESS regression is applied to the empirical data. The comparison of both curves is the base for the calibration procedure which is based on RMSE minimization. This would not be possible without using regression techniques. Secondly, the calibrated simulation is further used to estimate the MFD based on full trajectory data following Edie's definitions. By doing so, the impact of measurement induced biases on the shape of the MFD for the present case of the Leopoldstraße can be inspected.

3.4. Sensitivity analysis of signal and public transport parameters

The sensitivity analysis is conducted to study the impact of important input parameters of the analytical approximations on the resulting MFDs. The MoC does not allow for implementing varying green phases and cycle lengths within an intersection. The SA assumes green phases and cycle lengths which are independent and identically distributed. Both assumptions are violated by using the signal data at hand. Furthermore, the Leopoldstraße is frequented by buses of the public transport operator. To estimate the impacts of multimodal flows on the MFD by applying the approximation methods, additional data on public transport operation are required. However, no reliable data for the specific input parameters are currently available. Consequently, realistic assumptions are made.

We conduct a Monte-Carlo-Simulation to study the violation of assumptions concerning the signal related input parameters, as well as to analyze the assumption regarding public transport related input parameters. In order to replicate the real-world scenarios in the solution space, all possible input parameter combinations have to be considered. However, this is infeasible due to the high computational effort. To overcome this challenge, we apply a Latin Hypercube sampling to generate a representative range of values for each input parameter. Several scenarios are studied. In each scenario a different number and type of input parameter are varied. The studied input parameters are related to signal control and public transport operation. The signal related input parameters are drawn from the distribution of measured values. For the MoC, this includes the green time and cycle length ratio g/c, as well as the offset o. For the SA, the parameters considered for sampling are the average green time μ_g, the long-run red to green ratio ρ and the corresponding standard deviations. In order to derive according mean and standard deviation values, small samples of five consecutive cycles are considered. The sample size of five is chosen as a trade-off between having a large enough number of mean and standard deviation values for the Monte-Carlo-Simulation and avoiding extreme values for each mean and standard deviation. For the sake of simplicity, these parameters are also labeled g/c further on in the paper as they essentially refer to green times and cycle lengths. The public transport related input parameters consist of the bus frequency, the average speed v_b of buses for the MoC, and the average bus free flow speed u_b and dwell times t_d for the SA. However, no reliable data for these specific input parameters are available. Thus, the bus frequency is assumed to follow the schedule and is therefore not further investigated within the sensitivity study. Moreover, v_b and u_b are varied between 50 % and 100 % of the car free flow speed u. In addition, t_d is varied between 10 s and 60 s. The interval for t_d is chosen based on a limited number of on-site measurements.

For each input parameter, a sample with a size of $n = 10000$ is drawn. Based on a set of input parameters, the MFDs can be approximated for each scenario. The effects of varying input parameters are studied for both analytical methods, the MoC and the SA. To give an overview of the conducted scenarios, table 3 shows the investigated parameter combinations. As mentioned above, g/c represents the green phase and cycle length parameters for both the MoC and the SA. The input parameters o and v_b are only required for the MoC. The average bus free flow speed u_b and average dwell time t_d are only required for the SA.

Table 3: Input parameter configuration for the sensitivity study

	Method of cuts							Stochastic approximation						
Scenario	1	2	3	4	5	6	7	8	9	10	11	12	13	14
g/c	✓			✓	✓		✓	✓			✓	✓		✓
o		✓		✓		✓	✓							
v_b			✓		✓	✓	✓							
u_b									✓		✓		✓	✓
t_d										✓		✓	✓	✓

4. Results and discussion

This section shows and discusses the results for the case study, the investigation of the measurement bias and the sensitivity analysis. Many results are presented as MFDs, such as in Figure 4a, and Figure 5a - 8. If not stated otherwise, the abscissa shows the average density in veh/km/ln and the ordinate shows the average flow in veh/h/ln.

4.1. Case study

The results for the case study include the empirical MFD, and the MFDs approximated by the MoC the SA, respectively.

4.1.1. Empirical MFD

The empirical MFD is estimated based on the methods explained and the data described in the previous section. The result is shown in Figure 4a. The abscissa shows the average dimensionless occupancy per lane which ranges from 0 to 1. The figure shows a well-defined MFD with a clear shape. Especially, the data related to free flow states are little scattered. Maximum flows are observed around 480 veh/h/ln. These observations are similar to MFDs reported for other cities (e.g. Ambühl et al., 2017). The occupancy reaches values up to 0.6. At occupancies between 0.2 to 0.4, a clockwise hysteresis loop can be observed. Its investigation reveals that the upper part of the loop occurred during the loading period, while the lower part occurred during the unloading period in the evening. These periods correspond to the onset and offset of congestion. This pattern can be explained as follows. The direction of travel points towards the outer parts of the city, including the city's ring road. In other words, commuters are traveling along the Leopoldstraße to leave the city. This explains the time of the onset and offset of congestion. Similar patterns were observed in other studies (Saberi and Mahmassani, 2013; Buisson and Ladier, 2009). Reasons for this phenomenon are presented in Section 2.

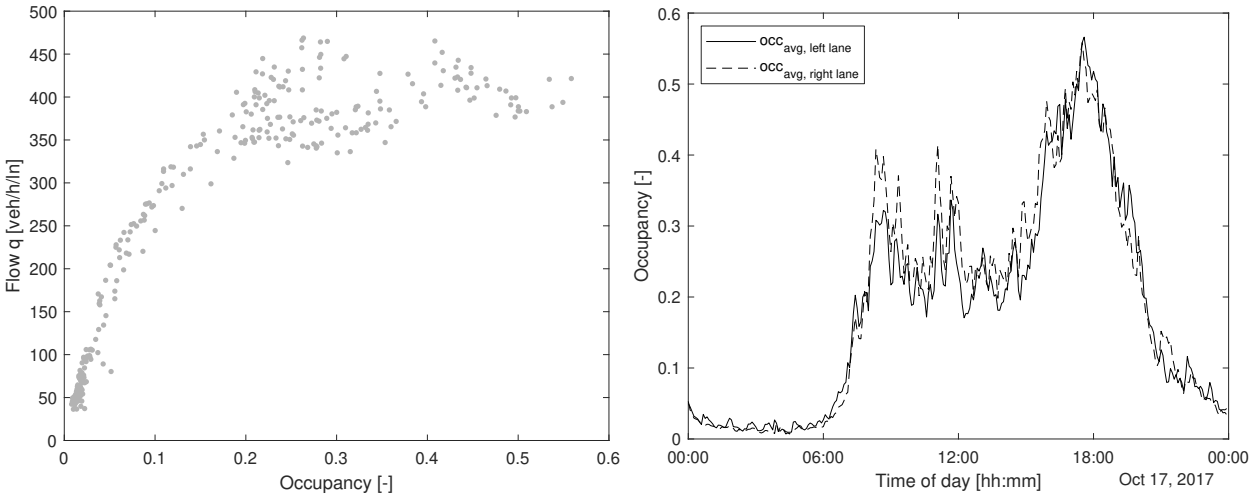

a) Empirically estimated MFD. **b)** Average lane-specific occupancies.

Figure 4: Empirical results for the Leopoldstraße on October 17, 2017.

The capacity of the arterial could be reduced due to constraining effects on the supply side (such as signals), but also due to demand-related matters. For example, if there were a strong favoring of one lane, the other lane's capacity might be underutilized and thus the MFD would not show the effective capacity for the whole road segment. To investigate this issue, we plot the lane specific average of occupancies for the analyzed road segment. The results are displayed in Figure 4b. The abscissa and the ordinate show the time

of day and the dimensionless occupancy per lane, respectively. The corresponding values for the left lane in direction of travel are shown as solid black curve, and as dashed black line for the right lane. The figure demonstrates that there are only minor differences between the two lanes. In general, occupancy values for the right lane are slightly higher than the ones for the left lane. Reasons for that might be the potentially higher frequency of flow-disturbing elements such as buses leaving a bus bay, cars looking for parking spots, and logistic vehicles while loading and unloading goods. However, the differences are minor and we thus conclude that the capacity of both lanes is utilized. Another reason for low flows apart from bottlenecks within the studied road segment can be constraining conditions upstream and downstream of the road segment. We suppose there are no upstream constraining conditions since we observe a congested branch in the empirical MFD. If there would be any constraining conditions upstream, the observed congested branch would be very limited. This is not the case, as can be seen in Figure 4a. Additionally, traffic flow could be constrained by spillbacks from downstream intersections. Unfortunately, the available data does not include measurements from such locations. However, qualitative on-site evaluation from several days suggests that spillbacks are rare and do not systematically impact the capacity of the most downstream intersection of the studied road segment of the Leopoldstraße. Comparable results for the time series of occupancies are found for other weekdays at the studied road segment. Additionally, the distribution of green times and cycle lengths in a second available data set do not substantially differ to the one shown in the paper. Thus, we assume that analyzing the data presented in the paper is representative for the given road segment. In summary, we assume that the observed capacity in the MFD is due to bottlenecks within the investigated system and not due to underutilized lanes or constraining impacts from up- or downstream.

4.1.2. Analytical approximation

The evaluation of the analytical approximations for a given set of input parameters leads to an estimate for the upper bound of the MFD, shown in Figure 5. The curves show the MFDs estimated based on the MoC and the SA. For comparison, the scatter plot is shown too, representing the empirically derived MFD with occupancies converted to densities as described in Section 3. The general trapezoidal shape results from the fact that the MoC and SA approximate the MFD based on different families of cuts, as explained in Section 2.

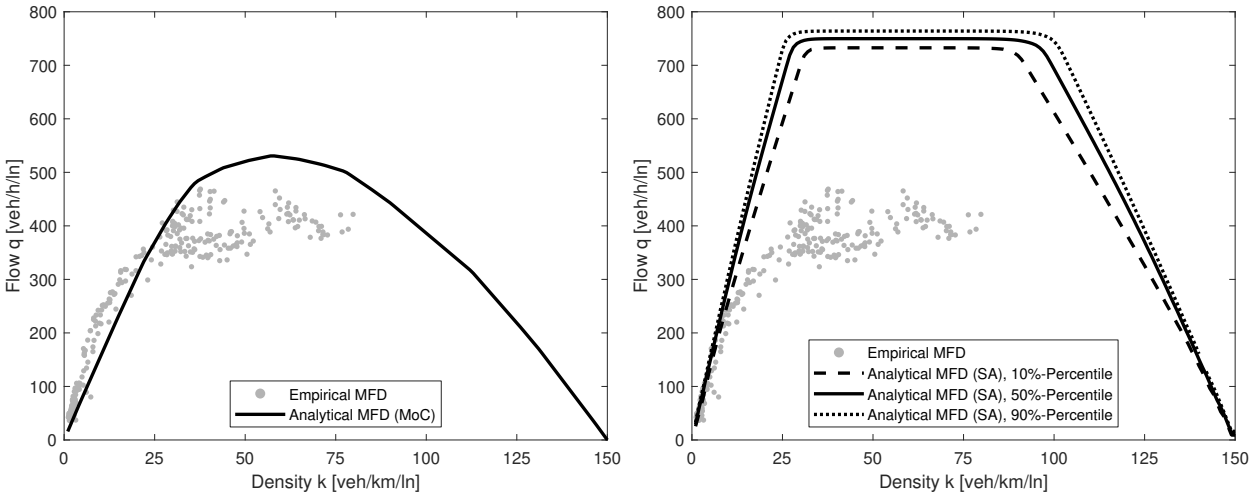

a) The MFD based on the MoC.

b) The MFD based on the SA.

Figure 5: Comparison of analytical approximated and empirically derived MFDs.

A qualitative comparison of the analytical MFD based on the MoC (see Figure 5a) and the empirical MFD leads to the following observations. The analytically derived free flow cut matches the data rather well, even though the flows are in general underestimated for densities ranging up to 25 veh/km/ln. For

densities greater than that, flows are overestimated by the MoC. Moreover, the maximum flow is reached around 470 veh/h/ln in reality. The estimated capacity of the MoC is around 530 veh/h/ln. Therefore, the MoC overestimates the capacity of the arterial by roughly 13 %. Possible reasons for such differences between the empirically estimated and the analytically approximated MFD are the assumptions related to the KWT such as instantaneous acceleration and stationary traffic flow. Short green times and cycle lengths could lead to an enhancement of the effects of these assumptions. Furthermore, taking the average of green times and cycle lengths as input to the MoC might decrease its accuracy. Moreover, the MoC does not allow for consideration of signal actuation or transit signal priority, which are in operation in reality and affect the traffic flow dynamics. Furthermore, the empirical MFD is based on LDD and thus includes a measurement bias. This bias is analyzed within this paper too. The respective results are presented in the next section. All these points potentially contribute to the observed discrepancies in the empirical estimated and analytical approximated MFD.

Please note that the SA computes a CDF for the MFD, i.e. a distribution of flows q for each density k. The results of the evaluation of the SA for the 10 %-, the 50 %- and the 90 %-percentile are shown in Figure 5b. Additionally, the figure shows the empirical data for comparison. The dashed, solid and dotted curves are the 10 %-, the 50 %- and the 90 %-percentile of the CDF of the MFD, respectively. Generally, the free flow branch of the analytical approximations fit the empirical data well up to a flow of about 250 veh/h/ln. For higher flows, differences arise. The largest discrepancy occurs for the capacity which is about 300 veh/h/ln, or about 63 % in relative terms. This discrepancy clearly exceeds the one observed for the MoC. Moreover, the difference between the percentiles of the analytical approximations are minor and cannot represent the scatter in the empirical data. The largest differences between them occur close to capacity and for the backward waves. We suppose that there exist several possible reasons for the large differences in the estimated and observed capacities. The actuated traffic signal control and transit signal priority violate the assumption of an independent distribution of green and red times. Moreover, there exist substantial differences in green-time-to-cycle-length ratios between intersections as can be concluded from Figure 3. In other words, intersection no. 3 has the lowest g/c ratio and, thus, is determining the overall capacity of the arterial. However, the SA derives the capacity cut based on an average of capacities related to each intersection. In the present case of an arterial with substantial differences of capacities within the intersections, this might lead to a wrong estimation of the overall capacity. Lastly, it is again noteworthy to mention that the empirical data includes a measurement bias which impacts the general fit. All in all, these aspects could lead to the fact that the capacity based on stationary cuts is overestimated.

To quantify the comparison of the MoC and the SA to the empirical MFD, the corresponding RMSE are calculated. For the MoC an RMSE of 83.0, and for the SA an RMSE of 271.2 is calculated. These values indicate that the overall approximation based on the MoC is superior to one based on the SA for the input parameter configuration of the case study. As mentioned above, probable reasons are related to the measurement bias included in empirical data, the representation of signal control and public transport operation in the models, as well as assumptions inherited from the KWT. The results of a thorough analysis of these aspects are investigated in the next subsections.

4.2. Investigation of the measurement bias

Since only limited empirical data are available, the associated measurement bias can only be estimated. This is done based on a microscopic simulation, as described in Section 3. Figure 6 shows the results of this investigation. Three different MFDs are presented. First, the MFD based on empirical LDD (ELDD) as presented in Figure 4a is displayed again as grey scatter plot for comparison. Additionally, the curve resulting from a LOESS regression based on this data is shown as black solid line. Secondly, the curve resulting from a LOESS regression based on virtual loop detector measurements (VLDD) is shown as black dotted line. The curve suggests flows $q > 0$ veh/h/ln for densities $k = 0$ veh/km/ln. Please note that this is a result of the regression method, and physically impossible. Lastly, the LOESS regression curve based on trajectories from the simulation, virtual floating car data (VFCD), is presented as black dashed line.

The regression results based on ELDD and VLDD were used for calibration. The RMSE of the LOESS (ELDD) and LOESS (VLDD) is 22 veh/h/ln. Considering the impact of day-to-day variance in traffic flow,

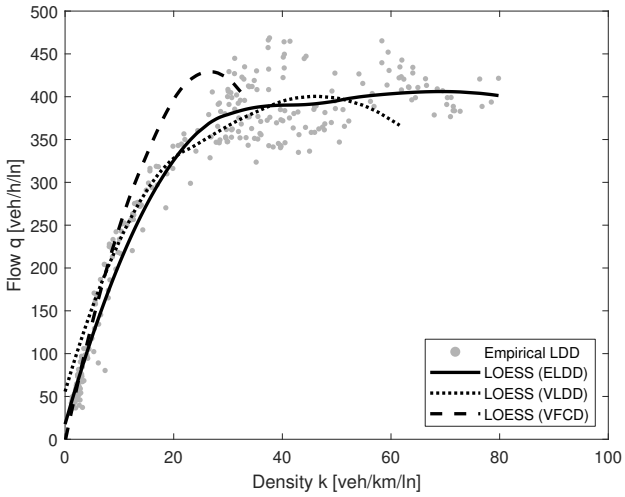

Figure 6: Illustration of the measurement bias estimation.

measurement errors and other factors we assume that this value is low enough for stating that the microscopic simulation is calibrated well enough for our purposes.

Since the trajectories contain all information, the curve based on virtual trajectories represents an estimate for an MFD without the measurement bias. It can be seen that the free flow branch is slightly shifted towards higher speeds and the capacity is increased by roughly 40 veh/h/ln. This means that the measurement bias could lead to an underestimation of the actual measured capacity, and thus the error of the analytical approximation could be smaller as observed by comparison with the empirical LDD based MFD. Furthermore, the results indicate that the average free flow speed in the network is underestimated by simply relying on the empirical data.

4.3. Sensitivity analysis of signal and public transport parameters

As discussed before based on the results from the case study, the representation of signal control schemes and public transport operation in the analytical approximations are potential reasons for the differences of the corresponding MFDs and the empirical MFD. In order to study the impact of the related input parameters, a Monte-Carlo-Simulation with $n = 10000$ draws is conducted as described in Section 3. Thus, for each density value a range of 10000 flow values is calculated. Based on these results, a corresponding minimum q_{min}, mean q_{mean} and maximum flow q_{max} can be derived. For the whole range of densities, these flows can be plotted as curves. Each curve is compared to the empirical MFD and an RMSE is calculated. The following subsections show and discuss the results for both investigated analytical approximations. The data plotted in Figure 7 and Figure 8 show the empirical MFD as scatter plot, and q_{min}, q_{mean} and q_{max} as dashed, solid and dotted curve, respectively.

4.3.1. Method of cuts

Three input parameters of the MoC are related to signal control and public transport operation. This is the green time and cycle length which is represented by g/c, the offsets o and the average bus speed v_b. To investigate all parameters and the possible combinations of them, seven scenarios are studied. Presenting all plots within this paper is not expedient since the generally observed patterns can be explained with the three diagrams shown in Figure 7.

As expected, varying the parameter g/c related to cycle length and green times has a large impact on the shape of the resulting MFDs (see Figure 7a). The capacity ranges between roughly 200 veh/h/ln and 800 veh/h/ln. Additionally, the free flow and congested branches of the MFD are varying strongly. Interestingly, the mean flows q_{mean} approximate the empirical MFD well. Figure 7b shows the results of

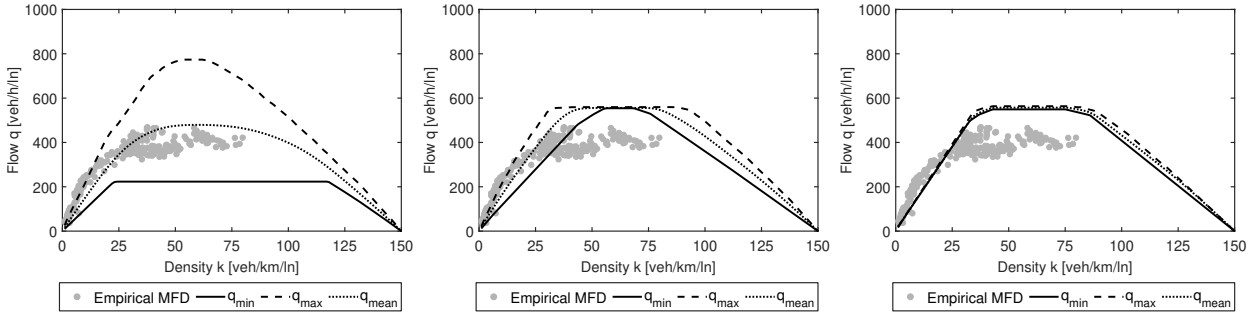

a) Scenario 1: Sensitivity to g/c. **b)** Scenario 2: Sensitivity to o. **c)** Scenario 3: Sensitivity to v_b.

Figure 7: Results of the sensitivity analysis of the MoC.

the sensitivity analysis of the input parameter related to the offset o. As expected, the impact on capacity is negligible. However, the free flow and congested branches are highly impacted by this input parameter. In general, the offset is challenging to specify, since it is adaptive in reality and this cannot be reproduced by the MoC. Lastly, Figure 7c presents the results for the scenario related to the average bus speed v_b. It can be seen that the impact is minor. Thus, for the current representation of public transport in the MoC, this parameter plays only a minor role for the given case. Thus, assuming a corresponding value instead of measuring it is not crucial for the final result.

The figures for the other four scenarios (4 to 7) are not shown explicitly. Generally, visual inspection shows that the parameter g/c has the major influence also when it is combined with the other studied input parameters. The combination of o and v_b reveals that their impact on the MFD is still minor in comparison to g/c. Thus, the main shapes of the results are similar to the ones shown in Figure 7. For the sake of comprehensiveness, the numerical results in the form of RMSE for all scenarios are presented in Table 4.

Table 4: RMSE results for the sensitivity study of the MoC

Scenario	RMSE		
	q_{min}	q_{mean}	q_{max}
1	138.1	59.2	224.8
2	88.1	104.3	123.8
3	106.5	111.2	117.7
4	141.1	59.3	228.6
5	138.8	58.5	225.0
6	83.7	104.8	127.7
7	140.8	58.7	230.1

The results for the RMSE reveal further insights. First, it can be seen that the calculated RMSE for q_{mean} are the smallest except for scenario 2 and 6. q_{mean} for sceanrios 1, 4, 5 and 7 have a lower RMSE than the one calculated for the MFD of the case study. Thus, using q_{mean} would lead to an improved estimation of the empirical MFD for these scenarios. Another interesting result is that the RMSE of q_{mean} differ from the one related to the case study. In the case study, the MoC was applied with the average of each input parameter. Comparing the RMSE from resulting MFD from the case study to the RMSE of q_{mean} resulting from the sensitivity study reveals a difference. That is that the average input values do not lead to the mean output values. This finding confirms the purposefulness of the sensitivity study. Moreover, the ranges between the RMSE of q_{min} and q_{max} differ greatly. They are especially large when the parameter g/c is varied, such as in scenario 1, 4, 5 and 7. This lets us conclude that the impact of g/c is the largest on

the analytical approximation by the MoC. This is in line with what was concluded from Figure 7a. Lastly, the low impact of the average bus speed v_b is evident when the corresponding RMSE values are studied for scenario 3. Additionally, the values for scenario 5 are similar to the ones of scenario 1, so the interactive effect of v_b with g/c is low. The same applies to scenarios 2 and 6, where the interactive effect of v_b with o is examined.

In summary, it can be observed that the approximated capacity is highly sensitive to g/c. This is an expected result. However, averaging the flows for each density based on the computed MFD approximations reveals a well-fitting curve to the empirical MFD. This is interesting, since possible g/c values can be estimated based on signal control programs and thus an ex-ante prediction of the capacity of the arterial is feasible. The high sensitivity to g/c is due to the direct relation of this parameter to the stationary cut which affects the capacity for the present case. The choice of offsets o has a substantial impact on the free flow and backward wave branch but no effect on the capacity of the resulting MFDs. Reasons for that are varying offsets o do not affect the g/c ratio and thus not the capacity, as long as the stationary cuts are constraining. However, different offsets change the variational graph in such a way that the impact on shortest paths within the framework of the MoC leads to differing free flow and backward wave branches in the resulting MFDs. The fit of these branches to empirical data or potentially bias-free data is limited. However, this is not surprising since only fixed-time control can be implemented into the MoC, whereas in reality traffic signal actuation and transit signal priority are in operation. Additionally, it is clearly shown that the public transport operation as currently implemented in the methods has nearly no effect on the resulting MFD. This can be due to the low impact on the variational graph for the given headway and average bus speed.

4.3.2. Stochastic approximation

Similar to the MoC, three input parameters are related to signal control and public transport operation for the SA. Similar to the MoC, g/c reflects the green time and cycle length, the dwell times of buses t_d and the average bus free flow speed u_b. Again, seven different scenarios are studied to investigate all parameters and their possible combinations. Since the SA calculates a CDF of the MFD, a percentile has to be specified to derive a single MFD for each run within the sensitivity analysis. We choose the 50 %-percentile as this seems to be the most representative.

Visual inspection of all plots shows again that it is sufficient to present only the diagrams of the first three scenarios in Figure 8. The main results can be explained through these figures.

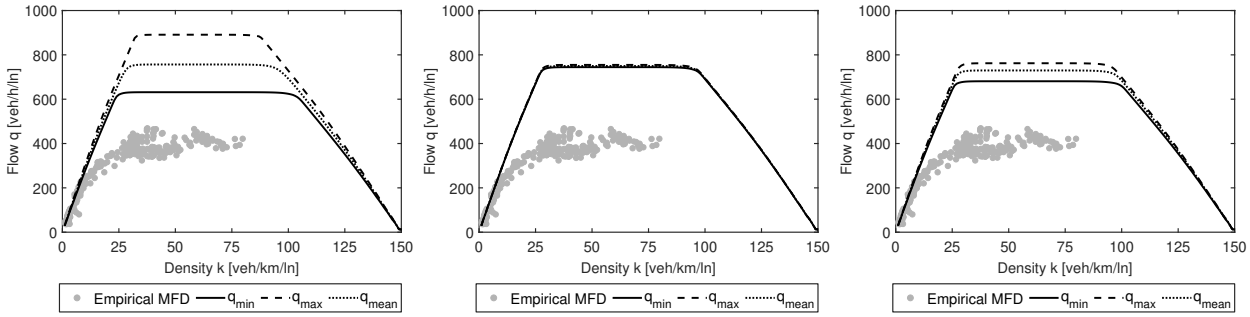

a) Scenario 8: Sensitivity to g/c. **b)** Scenario 9: Sensitivity to t_d. **c)** Scenario 10: Sensitivity to u_b.

Figure 8: Results of the sensitivity analysis of the SA.

Figure 8a shows that the parameter g/c related to cycle length and green times has again a large impact on the shape of the resulting MFDs. The capacity ranges roughly between 600 veh/h/ln and 900 veh/h/ln. Contrarily to the results of the MoC, the free flow and congested branch of the MFD are barely affected. Figure 8b shows the results for varying the bus dwell times. It becomes clear that this input parameter has a negligible influence on the MFD for the investigated case. Thus, it seems that the choice of this parameter is not important for applying the SA for the case of the Leopoldstraße. Lastly, Figure 8c presents the results for

the scenario related to the average bus free flow speed u_b. The parameter has a substantial influence on the shape of the MFD. More specifically, it can be seen that the capacity ranges between 650 and 750 veh/h/ln. For all figures, it is observed that the free flow and backward wave regions are substantially less impacted by varying the input parameters compared to the MoC. Since the free flow cut matches the empirical data well, this is an advantage of the SA.

Again, the figures for the other four scenarios (10 to 14) are not shown explicitly. Visual inspection reveals that no unexpected interaction effects between the studied input parameters exist. The consideration of multiple variable input parameters results in adding their impacts. For example, t_d has still very limited effects when it is combined with g/c or u_b. The main shapes of the results are similar to the ones shown in Figure 8. For the sake of comprehensiveness, the numerical results in the form of RMSE for all scenarios are presented in Table 5.

Table 5: RMSE results for the sensitivity study of the SA

Scenario	RMSE		
	q_{min}	q_{mean}	q_{max}
8	267.5	271.2	274.8
9	187.2	275.7	367.5
10	221.6	256.8	280.2
11	204.3	256.6	293.7
12	148.9	261.0	369.7
13	174.6	275.5	372.0
14	133.7	260.9	369.7

The results for the RMSE reveal further insights. First, it can be seen that the calculated RMSE for q_{min} are always the smallest. Additionally, all q_{min} have a lower RMSE than the one calculated for the MFD of the case study. Thus, using q_{min} would lead to an improved estimation of the empirical MFD for all scenarios. Another interesting result is that the RMSE of q_{mean} differ from the one related to the case study. Similarly to the results for the MoC, the mean input to the SA does not lead to the mean output. Moreover, the ranges between the RMSE of q_{min} and q_{max} differ greatly. They are especially large when the parameter g/c is varied, such as in scenario 8, 11, 12 and 14. This lets us conclude that the impact of g/c is the largest on the analytical approximation by the SA. This is in line with what was concluded from Figure 8a and with similar results for the MoC. Lastly, the low impact of the bus dwell times t_d is evident when the corresponding RMSE values are studied for scenario 10. Additionally, the values for scenario 12 are similar to the ones of scenario 10, so the interactive effect of u_b with g/c is low. The same applies to scenarios 10 and 13, where the interactive effect of u_b with t_d is examined.

Generally, the SA shows a good and robust fit to the free flow branch. However, the capacity is clearly overestimated, even by taking the minimum of all computed MFDs in the corresponding scenarios. Reasons for such an overestimation are discussed in Section 4.1.2. Nevertheless, the method seems to capture public transport operation more effectively, since the related parameters have a substantial impact on the resulting MFDs. This could be due to the endogenous consideration of effective bus speeds in the model (Castrillon and Laval, 2017). Extending the SA to account for single intersections which dominate the overall capacity might be an interesting line of research. Such an extension could lead to a better fit to empirical data for cases similar to the Leopoldstraße, i.e. arterials with a comparably low number of intersections and high variability in signal timings.

This study aimed to investigate the differences between the empirically estimated and analytically approximated MFDs. The results shed light on possible reasons, such as the measurement bias, model assumptions and simplified consideration of signal control and public transport operation. Remaining unexplored reasons for discrepancies are likely the assumptions of the KWT, and the hysteresis phenomenon. For example, the role of infinite acceleration and deceleration implied by KWT could be investigated. First analyses con-

ducted by the authors showed that more effort is necessary to understand the effect of these parameters on the MFD. Setting the acceleration and deceleration to extremely high values in the car-following model of the microscopic simulation does not produce the expected results. Under such conditions, some vehicles are not able to perform lane changes to reach their desired destination. As a result, they remain stopped at intersections. This causes unnecessary congestion, reduces the capacity of the arterial, and increases the differences between the simulation-based and analytical MFDs. Since a more detailed investigation of this phenomenon is beyond the scope of this paper, we suggest future research to study the role of infinite acceleration assumption of KWT. The hysteresis phenomenon can be considered with MFD-based modeling as shown in Mariotte et al. (2017). However, both the MoC and SA are methods to derive accumulation-based MFDs and thus such an investigation lies beyond the scope of this paper. Overall, the conducted analysis helps to gain a better understanding of several potential error sources.

5. Conclusion

This paper compares two different methods which analytically approximate the arterial MFD. The first method is the MoC which is based on the KWT. It is deterministic and approximates the MFD based on the link FD, road topology, signal settings and public transport operation parameters. The second method is the SA. It considers the stochasticity of input parameters and estimates a CDF for the MFD. Within a case study, both methods are evaluated by comparing the resulted MFDs against the MFD derived from empirical data collected at five intersections of an urban arterial, namely the Leopoldstraße in Munich, Germany. The empirical data set consists mainly of LDD and time-stamps for signal phase changes. The case study reveals differences between the empirical and analytical MFDs. Subsequently, the paper investigates potential reasons for the occurring discrepancies between the empirical estimation of the MFD and corresponding analytical approximations. This includes the analysis of the measurement bias which is induced by LDD. The results suggest that the actual capacity could be larger as the empirical MFD proposes for the studied case. Moreover, the free flow branch of the estimated MFD appears to be steeper without the bias. Eventually, an in-depth investigation of the input parameters regarding signal control and public transport operation for both methods and their impacts on the resulting MFD approximation is conducted. The analysis is performed as Monte-Carlo-Simulation based on a Latin Hypercube sampling. The results indicate that the capacity predicted by both methods is highly sensitive to the green-to-cycle ratio related input parameters. Interestingly, the mean flow resulting from calculating a large sample of MFDs based on the MoC by varying the green-to-cycle ratio fits the empirical data very well. Moreover, the offsets have a strong impact on the free flow branch of MFDs predicted by the MoC, which is generally underestimated by this method. Contrarily, the SA overestimates the capacity for all cases. However, this method predicts the free flow branch accurately. Input parameters related to public transport operation have a comparably minor impact. Overall, the MoC seems to be more promising for the case studied within this paper as indicated by the corresponding RMSE results. By knowing possible green-to-cycle ratios, a general shape of the MFD seems to be predictable for highly inhomogeneous urban arterials. This opens the door to model-predictive traffic control based on the MFD.

The contributions of this paper include an in-depth analysis of the role of signal data for analytical MFD estimation methods. Moreover, we compare the performance of two prominent analytical MFD estimation methods to empirical data from an arterial in Munich, Germany. The results indicate that the MoC can be applied to estimate the capacity for highly inhomogeneous arterials, whereas the SA delivers a good fit for the free-flow branch.

Future research regards to investigate more urban arterials to generalize the findings for the MoC and the SA. Furthermore, extending the MoC to be applicable to road networks and arterials with traffic actuated signal control would be an interesting task. This could lead to a fast and efficient way to analyze the capacity of an arterial with actuated signal control. Thus, it could be used to study different signal control strategies regarding maximum arterial capacity. However, it is unclear if the mathematical framework holds for hyperlinks which represent varying signal timings between intersections and at each intersection to represent more complex signal control schemes. Thus, completely new approaches might be necessary.

Nevertheless, more accurate implementation of public transport can be incorporated. This might already improve the accuracy of the methods. Moreover, only the SA applies to networks. No deterministic method such as the MoC is available to analytically estimate the MFD for networks in general. The MoC was only applied to simplified networks, which can be approximated by a single arterial. Therefore, corresponding developments could open the door to network-wide deterministic ex-ante MFD prediction.

Acknowledgments

The authors would like to express their gratitude to Prof. Ludovic Leclercq and Prof. Jorge Laval for providing the MATLAB® and Mathematica® codes for their methods. Furthermore, the authors would like to thank the KVR of Munich for providing the data this study is based on. Lastly, we would like to thank the anonymous reviewers for their valuable comments which helped to substantially improve the paper.

References

Aboudolas, K., Geroliminis, N., 2013. Perimeter and boundary flow control in multi-reservoir heterogeneous networks. Transportation Research Part B: Methodological 55, 265–281. doi:10.1016/j.trb.2013.07.003.

Ambühl, L., Loder, A., Bliemer, M.C., Menendez, M., Axhausen, K.W., 2018. A functional form with a physical meaning for the macroscopic fundamental diagram. Transportation Research Part B: Methodological doi:10.1016/j.trb.2018.10.013.

Ambühl, L., Loder, A., Bliemer, M.C., Menendez, M., Axhausen, K.W., 2018. Introducing a resampling methodology for the estimation of empirical macroscopic fundamental diagrams. Transportation Research Record: Journal of the Transportation Research Board 2676, 239–248.

Ambühl, L., Loder, A., Menendez, M., Axhausen, K.W., 2017. Empirical macroscopic fundamental diagrams: New insights from loop detector and floating car data, in: Presented at the 96th Annual Meeting of the Transportation Research Board.

Ambühl, L., Loder, A., Zheng, N., Axhausen, K.W., Menendez, M., 2019. Approximative network partitioning for mfds from stationary sensor data. Transportation Research Record: Journal of the Transportation Research Board 2673, 94–103. doi:10.1177/0361198119843264.

Ambühl, L., Menendez, M., 2016. Data fusion algorithm for macroscopic fundamental diagram estimation. Transportation Research Part C: Emerging Technologies 71, 184–197. doi:10.1016/j.trc.2016.07.013.

Amini, S., Tilg, G., Busch, F., 2018. Evaluating the impact of real-time traffic control measures on the resilience of urban road networks, in: 2018 21st International Conference on Intelligent Transportation Systems (ITSC), IEEE. pp. 519–524.

Arnet, K., Guler, S.I., Menendez, M., 2015. Effects of multimodal operations on urban roadways. Transportation Research Record: Journal of the Transportation Research Board 2533, 1–7. doi:10.3141/2533-01.

Batista, S., Leclercq, L., Geroliminis, N., 2019. Estimation of regional trip length distributions for the calibration of the aggregated network traffic models. Transportation Research Part B: Methodological 122, 192 – 217. doi:doi.org/10.1016/j.trb.2019.02.009.

Buisson, C., Ladier, C., 2009. Exploring the impact of homogeneity of traffic measurements on the existence of macroscopic fundamental diagrams. Transportation Research Record 2124, 127–136.

Cao, J., Menendez, M., 2015. System dynamics of urban traffic based on its parking-related-states. Transportation Research Part B: Methodological 81, 718–736. doi:10.1016/j.trb.2015.07.018.

Castrillon, F., 2015. Theoretical analysis of the effects of bus operations on urban corridors and networks. Ph.D. thesis. Georgia Institute of Technology.

Castrillon, F., Laval, J., 2017. Impact of buses on the macroscopic fundamental diagram of homogeneous arterial corridors. Transportmetrica B: Transport Dynamics 6, 286–301. doi:10.1080/21680566.2017.1314203.

Cleveland, W.S., 1979. Robust locally weighted regression and smoothing scatterplots. Journal of the American statistical association 74, 829–836. doi:10.1080/01621459.1979.10481038.

Courbon, T., Leclercq, L., 2011. Cross-comparison of macroscopic fundamental diagram estimation methods. Procedia-Social and Behavioral Sciences 20, 417–426. doi:10.1016/j.sbspro.2011.08.048.

Daganzo, C.F., 2005a. A variational formulation of kinematic waves: basic theory and complex boundary conditions. Transportation Research Part B: Methodological 39, 187–196. doi:10.1016/j.trb.2004.04.003.

Daganzo, C.F., 2005b. A variational formulation of kinematic waves: Solution methods. Transportation Research Part B: Methodological 39, 934–950. doi:10.1016/j.trb.2004.05.003.

Daganzo, C.F., 2007. Urban gridlock: Macroscopic modeling and mitigation approaches. Transportation Research Part B: Methodological 41, 49–62. doi:10.1016/j.trb.2006.03.001.

Daganzo, C.F., Gayah, V.V., Gonzales, E.J., 2011. Macroscopic relations of urban traffic variables: Bifurcations, multivaluedness and instability. Transportation Research Part B: Methodological 45, 278 – 288. doi:10.1016/j.trb.2010.06.006.

Daganzo, C.F., Geroliminis, N., 2008. An analytical approximation for the macroscopic fundamental diagram of urban traffic. Transportation Research Part B: Methodological , 771–781doi:10.1016/j.trb.2008.06.008.

Daganzo, C.F., Lehe, L.J., 2016. Traffic flow on signalized streets. Transportation Research Part B: Methodological 90, 56–69. doi:10.1016/j.trb.2016.03.010.

Daganzo, C.F., Lehe, L.J., Argote-Cabanero, J., 2018. Adaptive offsets for signalized streets. Transportation Research Part B: Methodological 117, 926–934. doi:10.1016/j.trb.2017.08.011.

Daganzo, C.F., Menendez, M., 2005. A variational formulation of kinematic waves: Bottleneck properties and examples, in: Proceedings of the 16th International Symposium on Transportation and Traffic Theory.

Dakic, I., Menendez, M., 2018. On the use of lagrangian observations from public transport and probe vehicles to estimate car space-mean speeds in bi-modal urban networks. Transportation Research Part C: Emerging Technologies 91, 317–334. doi:10.1016/j.trc.2018.04.004.

Department for Transport, 2015. Free flow vehicle speeds statistics: Great Britain 2014. Technical Report October. Department for Transport, UK.

Du, J., Rakha, H., Gayah, V.V., 2016. Deriving macroscopic fundamental diagrams from probe data: Issues and proposed solutions. Transportation Research Part C: Emerging Technologies 66, 136–149. doi:10.1016/j.trc.2015.08.015.

Duruisseau, C., Leclercq, L., 2018. A Global Sensitivity Analysis of Dynamic Loading and Route Selection Parameters on Network Performances. Journal of Advanced Transportation 2018. doi:https://doi.org/10.1155/2018/8414069.

Edie, L., 1963. Discussion of traffic stream measurements and definitions, in: Almond, J. (Ed.), Proceedings of the 2nd International Symposium on the Theory of Traffic Flow, OECD, Paris, France. pp. 139–154.

Gayah, V., Daganzo, C.F., 2011. Clockwise hysteresis loops in the Macroscopic Fundamental Diagram: An effect of network instability. Transportation Research Part B: Methodological 45, 643–655. doi:10.1016/j.trb.2010.11.006.

Gayah, V.V., Gao, X., Nagle, A.S., 2014. On the impacts of locally adaptive signal control on urban network stability and the Macroscopic Fundamental Diagram. Transportation Research Part B: Methodological 70, 255–268. doi:10.1016/j.trb.2014.09.010.

Geroliminis, N., Boyacı, B., 2012. The effect of variability of urban systems characteristics in the network capacity. Transportation Research Part B: Methodological 46, 1607–1623. doi:10.1016/j.trb.2012.08.001.

Geroliminis, N., Daganzo, C.F., 2008. Existence of urban-scale macroscopic fundamental diagrams: Some experimental findings. Transportation Research Part B: Methodological 42, 759–770. doi:10.1016/j.trb.2008.02.002.

Geroliminis, N., Haddad, J., Ramezani, M., 2012. Optimal perimeter control for two urban regions with macroscopic fundamental diagrams: A model predictive approach. IEEE Transactions on Intelligent Transportation Systems 14, 348–359.

Geroliminis, N., Sun, J., 2011. Hysteresis phenomena of a macroscopic fundamental diagram in freeway networks. Transportation Research Part A: Policy and Practice 45, 966–979. doi:10.1016/j.tra.2011.04.004.

Geroliminis, N., Zheng, N., Ampountolas, K., 2014. A three-dimensional macroscopic fundamental diagram for mixed bi-modal urban networks. Transportation Research Part C: Emerging Technologies 42, 168–181.

Girault, J.T., Gayah, V.V., Guler, I., Menendez, M., 2016. Exploratory analysis of signal coordination impacts on macroscopic fundamental diagram. Transportation Research Record: Journal of the Transportation Research Board , 36–46doi:10.3141/2560-05.

Godfrey, J., 1969. The mechanism of a road network. Traffic Engineering & Control 8.

Grigoropoulos, G., Keler, A., Kaths, J., Kaths, H., Spangler, M., Hoffmann, S., Busch, F., 2018. Evaluation of the traffic efficiency of bicycle highways: A microscopic traffic simulation study, in: Presented at the 7th Symposium of the European Association for Research in Transportation.

Herman, R., Prigogine, I., 1979. A two-fluid approach to town traffic. Science 204, 148–151.

Ji, Y., Daamen, W., Hoogendoorn, S., Hoogendoorn-Lanser, S., Qian, X., 2010. Investigating the Shape of the Macroscopic Fundamental Diagram Using Simulation Data. Transportation Research Record: Journal of the Transportation Research Board 2161, 40–48. doi:10.3141/2161-05.

Keyvan-Ekbatani, M., Kouvelas, A., Papamichail, I., Papageorgiou, M., 2012. Exploiting the fundamental diagram of urban networks for feedback-based gating. Transportation Research Part B: Methodological 46, 1393–1403.

Knoop, V.L., De Jong, D., Hoogendoom, S.P., 2014a. Influence of road layout on network fundamental diagram. Transportation Research Record 2421, 22–30.

Knoop, V.L., de Jong, D., Hoogendoorn, S.P., 2014b. The influence of the road layout on the network fundamental diagram. Transportation Research Record: Journal of the Transportation Research Board 2421, 22–30. doi:10.3141/2421-03.

Knoop, V.L., van Lint, H., Hoogendoorn, S.P., 2015. Traffic dynamics: Its impact on the macroscopic fundamental diagram. Physica A: Statistical Mechanics and its Applications 438, 236–250. doi:10.1016/j.physa.2015.06.016.

Kouvelas, A., Saeedmanesh, M., Geroliminis, N., 2017. Enhancing model-based feedback perimeter control with data-driven online adaptive optimization. Transportation Research Part B: Methodological 96, 26 – 45. doi:doi.org/10.1016/j.trb.2016.10.011.

Krauß, S., 1998. Microscopic modeling of traffic flow: Investigation of collision free vehicle dynamics. Ph.D. thesis.

Laval, J.A., Castrillón, F., 2015. Stochastic approximations for the macroscopic fundamental diagram of urban networks. Transportation Research Part B: Methodological 81, 904–916. doi:10.1016/j.trb.2015.09.002.

Leclercq, L., 2005. Calibration of flow–density relationships on urban streets. Transportation Research Record: Journal of the Transportation Research Board 1934, 226–234. doi:10.1177/0361198105193400124.

Leclercq, L., Chiabaut, N., Trinquier, B., 2014. Macroscopic fundamental diagrams: A cross-comparison of estimation methods. Transportation Research Part B: Methodological 62, 1–12. doi:10.1016/j.trb.2014.01.007.

Leclercq, L., Geroliminis, N., 2013. Estimating mfds in simple networks with route choice. Transportation Research Part B Methodological 57, 468–484. doi:10.1016/j.trb.2013.05.005.

Leclercq, L., Sénécat, A., Mariotte, G., 2017. Dynamic macroscopic simulation of on-street parking search: A trip-based approach. Transportation Research Part B: Methodological 101, 268–282. doi:10.1016/j.trb.2017.04.004.

Lighthill, M.J., Whitham, G.B., 1955. On kinematic waves ii. a theory of traffic flow on long crowded roads. Proc. R. Soc. Lond. A 229, 317–345.

Loder, A., Ambühl, L., Menendez, M., Axhausen, K.W., 2017. Empirics of multi-modal traffic networks – using the 3d macroscopic fundamental diagram. Transportation Research Part C: Emerging Technologies 82, 88–101. doi:10.1016/j.trc.2017.06.009.

Loder, A., Ambühl, L., Menendez, M., Axhausen, K.W., 2019. Understanding traffic capacity of urban networks. Scientific reports 9, 1–10.

Lopez, C., Leclercq, L., Krishnakumari, P., Chiabaut, N., van Lint, H., 2017. Revealing the day-to-day regularity of urban congestion patterns with 3d speed maps. Scientific Reports 7, 1–11. URL: https//dx.doi.org/10.1038/s41598-017-14237-8, doi:10.1038/s41598-017-14237-8.

Lopez, P.A., Behrisch, M., Bieker-Walz, L., Erdmann, J., Flötteröd, Y.P., Hilbrich, R., Lücken, L., Rummel, J., Wagner, P., Wießner, E., 2018. Microscopic traffic simulation using sumo, in: The 21st IEEE International Conference on Intelligent Transportation Systems, IEEE.

Mahmassani, H., Williams, J.C., Herman, R., 1987. Performance of urban traffic networks, in: Proceedings of the 10th International Symposium on Transportation and Traffic Theory, pp. 1–20.

Mariotte, G., Leclercq, L., 2019. Flow exchanges in multi-reservoir systems with spillbacks. Transportation Research Part B: Methodological 122, 327 – 349. doi:doi.org/10.1016/j.trb.2019.02.014.

Mariotte, G., Leclercq, L., Laval, J.A., 2017. Macroscopic urban dynamics: Analytical and numerical comparisons of existing models. Transportation Research Part B: Methodological 101, 245–267. doi:10.1016/j.trb.2017.04.002.

Mazloumian, A., Geroliminis, N., Helbing, D., 2010. The spatial variability of vehicle densities as determinant of urban network capacity. Philosophical Transactions of the Royal Society A: Mathematical, Physical and Engineering Sciences 368, 4627–4647.

Mühlich, N., Gayah, V.V., Menendez, M., 2014. An examination of mfd hysteresis patterns for hierarchical urban street networks using micro-simulation, in: Presented at the 94th Annual Meeting of the Transportation Research Board.

Nagle, A., Gayah, V., 2014. Accuracy of networkwide traffic states estimated from mobile probe data. Transportation Research Record: Journal of the Transportation Research Board 2421, 1–11. doi:10.3141/2421-01.

OpenStreetMap contributors, 2019. Munich dump retrieved from https://planet.osm.org .

Ortigosa, J., Gayah, V.V., Menendez, M., 2017. Analysis of one-way and two-way street configurations on urban grid networks. Transportmetrica B: Transport Dynamics 1270, 1–21. doi:10.1080/21680566.2017.1337528.

Richards, P.I., 1956. Shock waves on the highway. Operations research 4, 42–51.

Saberi, M., Mahmassani, H., 2013. Hysteresis and capacity drop phenomena in freeway networks empirical characterization and interpretation. Transportation Research Record: Journal of the Transportation Research Board 2391, 44–55. doi:10.3141/2391-05.

Saberi, M., Mahmassani, H., Hou, T., Zockaie, A., 2014. Estimating network fundamental diagram using three-dimensional vehicle trajectories. Transportation Research Record: Journal of the Transportation Research Board 2422, 12–20. doi:10.3141/2422-02.

Saeedmanesh, M., Geroliminis, N., 2016. Clustering of heterogeneous networks with directional flows based on "snake" similarities. Transportation Research Part B: Methodological 91, 250–269. URL: https://dx.doi.org/10.1016/j.trb.2016.05.008, doi:10.1016/j.trb.2016.05.008.

Saeedmanesh, M., Geroliminis, N., 2017. Dynamic clustering and propagation of congestion in heterogeneously congested urban traffic networks. Transportation Research Part B: Methodological 105, 193 – 211. doi:10.1016/j.trb.2017.08.021.

Shim, J., Yeo, J., Lee, S., Hamdar, S.H., Jang, K., 2019. Empirical evaluation of influential factors on bifurcation in macroscopic fundamental diagrams. Transportation Research Part C: Emerging Technologies 102, 509–520.

Sirmatel, I.I., Geroliminis, N., 2018. Mixed logical dynamical modeling and hybrid model predictive control of public transport operations. Transportation Research Part B: Methodological 114, 325 – 345. doi:doi.org/10.1016/j.trb.2018.06.009.

Tilg, G., Amini, S., Busch, F., 2019. Arterial macroscopic fundamental diagram: A comparison of analytical approximations and empirical data from munich, in: Presented at the 98th Annual Meeting of the Transportation Research Board.

Tsubota, T., Bhaskar, A., Chung, E., 2014. Macroscopic fundamental diagram for brisbane, australia. Transportation Research Record: Journal of the Transportation Research Board 2421, 12–21. doi:10.3141/2421-02.

Wu, X., Liu, H.X., Geroliminis, N., 2011. An empirical analysis on the arterial fundamental diagram. Transportation Research Part B: Methodological 45, 255–266. doi:10.1016/j.trb.2010.06.003.

Xie, X., Chiabaut, N., Leclercq, L., 2013. Macroscopic fundamental diagram for urban streets and mixed traffic: Cross comparison of estimation methods. Transportation Research Record: Journal of the Transportation Research Board 2390, 1–10. doi:10.3141/2390-01.

Yang, K., Menendez, M., Zheng, N., 2019. Heterogeneity aware urban traffic control in a connected vehicle environment: A joint framework for congestion pricing and perimeter control. Transportation Research Part C: Emerging Technologies 105, 439 – 455. doi:doi.org/10.1016/j.trc.2019.06.007.

Yang, K., Zheng, N., Menendez, M., 2018. Multi-scale perimeter control approach in a connected-vehicle environment. Transportation Research Part C: Emerging Technologies 94, 32 – 49. doi:doi.org/10.1016/j.trc.2017.08.014. iSTTT22.

Yildirimoglu, M., Sirmatel, I.I., Geroliminis, N., 2018. Hierarchical control of heterogeneous large-scale urban road networks via path assignment and regional route guidance. Transportation Research Part B: Methodological 118, 106 – 123. doi:doi.org/10.1016/j.trb.2018.10.007.

Zheng, N., Rérat, G., Geroliminis, N., 2016. Time-dependent area-based pricing for multimodal systems with heterogeneous users in an agent-based environment. Transportation Research Part C: Emerging Technologies 62, 133–148. doi:10.1016/j.trc.2015.10.015.

Zhong, R., Chen, C., Huang, Y., Sumalee, A., Lam, W., Xu, D., 2018. Robust perimeter control for two urban regions with macroscopic fundamental diagrams: A control-lyapunov function approach. Transportation Research Part B: Methodological

117, 687 – 707. doi:doi.org/10.1016/j.trb.2017.09.008. tRB:ISTTT-22.
Zockaie, A., Saberi, M., Saedi, R., 2018. A resource allocation problem to estimate network fundamental diagram in heterogeneous networks: Optimal locating of fixed measurement points and sampling of probe trajectories. Transportation Research Part C: Emerging Technologies 86, 245–262. doi:10.1016/j.trc.2017.11.017.